THW/P7-02

Spontaneous Formation and Evolution of Nonlinear Energetic Particle Modes with Time-dependent Frequencies

B.N. Breizman 1), M.K. Lilley 2), S.E. Sharapov 3)

1) Institute for Fusion Studies, The University of Texas, Austin, Texas, 78712 USA
2) Department of Earth and Space Sciences, Chalmers University of Technology, 41296 Göteborg, Sweden
3) Euratom/CCFE Fusion Association, Culham Science Center, Abingdon, Oxfordshire OX14 3DB, UK

E-mail contact: breizman@mail.utexas.edu

Abstract. The near-threshold regimes of wave excitation by energetic particles reveal a rich family of nonlinear scenarios ranging from benign mode saturation to explosive behaviour. The choice between these scenarios depends on relaxation processes that restore the unstable distribution function. Our recent analysis shows that only the explosive behaviour is possible when drag dominates at the wave-particle resonance. As a result, the instability follows a 'hard' non-linear scenario in which the saturation level is insensitive to the initial growth rate. The explosive nonlinear regimes produce phase space holes and clumps. In previous work, description of such structures was limited to the case of small frequency deviations from the bulk plasma eigenfrequency. However, there are many observations of frequency sweeping events in which the change in frequency is comparable to the frequency itself. The need to interpret such phenomena requires a non-perturbative theoretical formalism, which this new work provides. The underlying idea is that coherent structures represent travelling waves in fast-particle phase space. A rigorous solution of this type is obtained for a simple one-dimensional model. This model captures the essential features of resonant particles in more general multidimensional problems. The presented solution suggests an efficient approach to quantitative modelling of actual experiments.

1. Bump-on-tail model and basic equations

Energetic particle instabilities in fusion plasmas usually involve wave-particle resonances. This naturally puts a spotlight on resonant particles in the related theoretical studies. The key aspects of resonant particle behavior are rather general, and they can be understood within a simple one-dimensional bump-on-tail model that exhibits the characteristic nonlinear scenarios [1] This model captures the essential features of resonant particles in more general

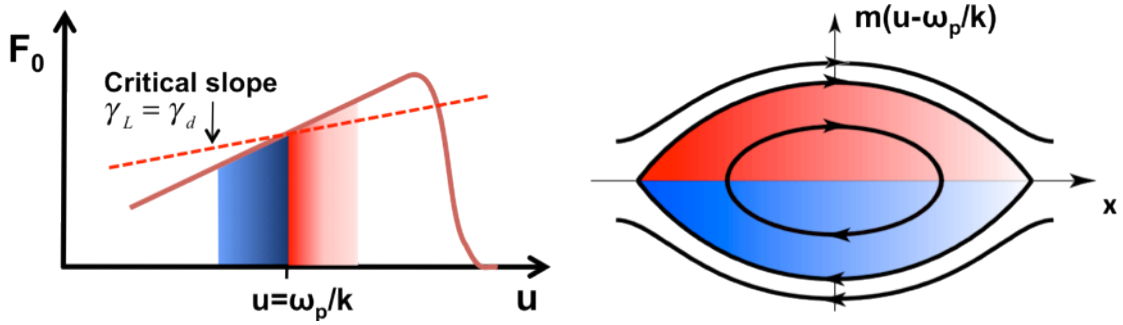

FIG. 1. Unstable bump-on-tail distribution function (left) and particle phase space plot (right).

multidimensional problems, because particle motion is known to be effectively one-dimensional in the vicinity of an isolated nonlinear resonance, once expressed in proper action-angle variables [2]. The bulk plasma is represented by cold electrons in the bump-on-

tail model, and the model includes sources and sinks that create an unstable energetic electron tail. The tail provides an instability drive γ_L due to positive slope of its velocity distribution function F (see *FIG. 1*). The unstable mode is a plasma wave, and its eigenfrequency, ω_p, is the electron plasma frequency. The cold electron collision frequency ν_{cold} provides a linear damping rate $\gamma_d = \nu_{cold}/2$ that determines the instability threshold (the minimum slope of $F(u)$ needed to excite a mode). The spectrum of energetic-particle-driven Alfvén modes in a tokamak is typically discrete due to periodicity in the toroidal and poloidal directions and the radial boundary conditions. In order to take that into account in the bump-on-tail model, we consider a single electrostatic mode with a given wavelength λ and wavenumber $k = 2\pi/\lambda$. The electric field of the mode can then be written as

$$E = \frac{1}{2}\left[\hat{E}(t)\exp(ikx - i\omega_p t) + \text{c.c.}\right], \tag{1}$$

where $\hat{E}(t)$ is slowly varying complex amplitude. The basic equations for the bump-on-tail problem are the kinetic equation for the energetic electrons and the wave evolution equation

$$\frac{\partial F}{\partial t} + u\frac{\partial F}{\partial x} + \frac{e}{2m}\left[\hat{E}(t)\exp(ikx - i\omega_p t) + \text{c.c.}\right]\frac{\partial F}{\partial u} = \left[\frac{\nu^3}{k^2}\frac{\partial^2}{\partial u^2} + \frac{\alpha^2}{k}\frac{\partial}{\partial u} - \beta\right]\left(F - F_0\right) \tag{2}$$

$$\frac{\partial \hat{E}}{\partial t} = -4\frac{\omega}{k}\pi e\int\left\langle F\exp(-ikx + i\omega_p t)\right\rangle du - \gamma_d\hat{E}, \tag{3}$$

where angular brackets denote averaging over wavelength. The right hand side of the kinetic equation describes three different collision models for the resonant tail electrons: velocity space diffusion, drag, and Krook-type collisions. The characteristic rates for these collisions are characterized by the quantities ν, α, and β, respectively. The collision operator also includes a source term that sets up an equilibrium distribution function F_0 in the absence of the wave field. The appropriate collision operator for the problem is determined by what collisional process is dominant at the wave-particle resonance in phase space. For fast ions in a tokamak, Coulomb collisions can be described as a combination of pitch angle scattering and electron drag. The former can be represented by a diffusive operator, while the latter introduces a slowing down operator to the kinetic equation.

2. Weakly nonlinear near-threshold dynamics

The near-threshold regime of wave excitation makes it possible to expand the perturbed distribution function F in powers of the wave amplitude $\hat{E}$ and solve the kinetic equation iteratively. The actual expansion parameter is $\omega_B t$, where $\omega_B \equiv \sqrt{e\left|\hat{E}\right|k/m}$ is the bounce frequency of the resonant particles, and t is the time interval of interest. The first term in the power series for F gives the linear instability drive $\gamma_L\hat{E}$ in the wave equation (3). The difference between γ_L and γ_d is small in the near threshold limit, which allows the lowest order nonlinear correction to compete with this difference. It follows from the expansion procedure that the nonlinear correction to the wave growth rate scales as $\gamma_L(\omega_B t)^4$ whereas the linear growth rate itself is $\gamma_L - \gamma_d << \gamma_L$. Consequently, the lowest order nonlinearity becomes important when $(\omega_B t)^4 \approx (\gamma_L - \gamma_d)/\gamma_L << 1$. At this level, the next-order nonlinear

term, $\gamma_L(\omega_B t)^8$, is still negligible. Thus, the inequality $(\gamma_L-\gamma_d)/\gamma_L \le (\omega_B t)^4 << 1$ defines a window in which the dynamics are already nonlinear but the nonlinearity can still be treated perturbatively. The ensuing relation between the perturbed distribution function and the wave field involves a sequence of time integrations. Once this relation is used in Eq. (3), we obtain a cubic integro-differential equation for the wave amplitude, which can be written in the following dimensionless form:

$$\frac{dA}{d\tau} = A(\tau) - \frac{1}{2}\int_0^{\tau/2} dz z^2 \int_0^{\tau-2z} dx \exp\left[-\hat{\nu}^3 z^2 (2z/3+x) - \hat{\beta}(2z+x) - i\hat{\alpha}^2 z(z+x)\right] \quad (4)$$
$$\times A(\tau-z)A(\tau-z-x)A^*(\tau-2z-x)$$

The amplitude A in this equation is defined as $A = (e\hat{E}k/m)(\gamma_L/\gamma_d - 1)^{-1/2}(\gamma_L-\gamma_d)^{-2}$, the dimensionless time is $\tau = (\gamma_L-\gamma_d)t$ and the normalized relaxation rates are defined as $\hat{\nu} \equiv \nu/(\gamma_L-\gamma_d)$, $\hat{\alpha} \equiv \alpha/(\gamma_L-\gamma_d)$, and $\hat{\beta} \equiv \beta/(\gamma_L-\gamma_d)$. The cubic nonlinear equation (4) was originally derived in Refs. [1, 3] for the diffusive and Krook-type collisions, and it has been generalized in Ref. [4] to include the effect of drag. Equation (4) determines whether the initial linear instability evolves into a soft or hard non-linear regime. The amplitude A saturates at a finite level in the soft case, whereas the hard case gives a solution that `explodes' in a finite time. In the absence of drag ($\hat{\alpha}=0$), Eq. (4) admits a saturated solution in which $|A|^2 = 2\left[\int_0^\infty \frac{z^2 dz}{\hat{\beta}+\hat{\nu}^3 z^2}\exp\left(-2\hat{\nu}^3 z^3/3 - 2\hat{\beta}z\right)\right]^{-1}$ at $\tau \to \infty$, and the amplitude indeed converges to that solution, but only when the annihilation rate ($\hat{\beta}$) and/or diffusion rate ($\hat{\nu}$) is sufficiently large. At smaller values of $\hat{\beta}$ and $\hat{\nu}$, the steady saturated solution is unstable, which gives rise to a periodic limit-cycle behaviour known as “pitchfork splitting”. Further decrease of the relaxation rates creates period doubling bifurcations and then leads to a chaotic mode amplitude evolution and to explosive growth of the mode. The details of these transitions can be found in Refs. [1, 5]. The same Eq. (4) also shows that the mode evolution is always explosive in the case of pure drag ($\hat{\beta}=\hat{\nu}=0$). The cubic nonlinear term in the equation is destabilizing in this case. Because of that, Eq. (4) does not have any saturated solution at ($\hat{\beta}=\hat{\nu}=0$), and the mode grows beyond the applicability range of Eq. (4). In presence of both drag and diffusion, the existence of steady saturated solutions is only prohibited when the integral in Eq. (4) has a negative real part at $\tau \to \infty$, which takes place at $\hat{\nu}/\hat{\alpha} < 1.043$ (as marked by the dashed line in figure 13). However, some of the steady solutions that formally exist at $\hat{\nu}/\hat{\alpha} > 1.043$ are in fact unstable [4]. The stability boundary is shown in *FIG. 2* by

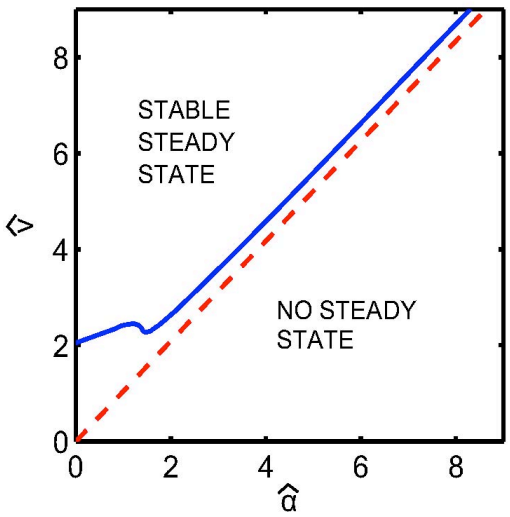

FIG. 2. The boundaries in parameter space that give stable, unstable and no steady state solutions to Eq. (4). The unstable solution lies in between the solid and dashed lines.

the solid line. The area above the solid line represents stable steady solutions. A distinctive feature of the explosive scenario is that the nonlinear growth rate of the wave in this regime is much greater than both the total linear growth rate $\gamma = \gamma_L - \gamma_d$ and the collisional relaxation rates of energetic particles. This rapid growth continues until the wave amplitude reaches the level of $\omega_B \approx \gamma_L$, at which point Eq. (4) looses its accuracy. The subsequent dynamics is governed by the fully nonlinear Eqs. (2) and (3). Their numerical solution in Ref. [6] has revealed formation of long-living coherent structures with time dependent frequencies (phase space holes and clumps). The next two sections present recent progress in the studies of such structures.

3. Phase space holes and clumps

The tendency for the mode frequency to change in the strongly nonlinear regime is already seen in the explosive solution of Eq. (4). The point is that the explosive solution is oscillatory, and the period of oscillations in the wave amplitude A shortens as the solution approaches the singularity. This nonlinear modulation of the growing wave suggests that the wave tends to split into upshifted and downshifted sidebands. The fully nonlinear set of Eqs. (2), (3) apparently prevents the mode from growing indefinitely (because of the energy conservation constraint). However, the trend for frequency sweeping continues, as found in Ref. [6]. There is a strong correlation between the frequency sweep and the evolution of the spatially averaged particle distribution function that exhibits an upward moving depletion (hole) and a downward moving protrusion (clump). The hole and clump represent resonant particles trapped in the field of the upshifted and downshifted waves, respectively. Unlike the very fast explosive formation of holes and clumps, their subsequent evolution takes place over many bounce periods of the trapped particles, so that these particles respond to the wave field adiabatically. Conservation of the adiabatic invariant preserves the value of the trapped particle distribution function. A schematic snapshot of the distribution function in *FIG. 3* shows that the particle kinetic energy decreases when the hole and clump move away from the original resonance with the constant values of the distribution function at the bottom of the hole and the top of the clump. This energy release balances the dissipation in the background plasma to allow the wave last over hundreds of linear damping times. As shown in Ref. [6], each hole and clump represents a nonlinearly saturated wave with

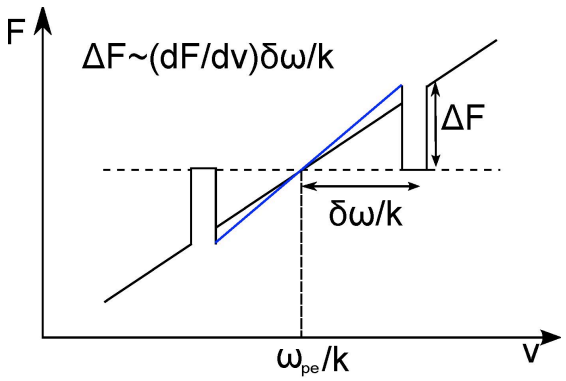

FIG. 3. Adiabatic motion of hole and clump releases kinetic energy of the energetic particles

$$\omega_B = \left(16/3\pi^2\right)\gamma_L \qquad (5)$$

and with the following square-root time-dependence for the frequency shift in the absence of fast particle collisions:

$$\delta\omega = \left(16/3\pi^2\right)\gamma_L\sqrt{2\gamma_d t/3}\,. \qquad (6)$$

More recent simulations with improved computational accuracy [7] reveal that holes and

clumps are produced continuously in the collisionsless case. This occurs due to the 'wake' that forms when a hole or clump detaches from the original resonance. Referring to *FIG. 3*, since the particle number is conserved, the motion of a hole or clump leads to slight excess behind a hole and depletion behind a clump. There is thus a tendency for the slope of the distribution function to steepen, making the system susceptible to recurrent instability.

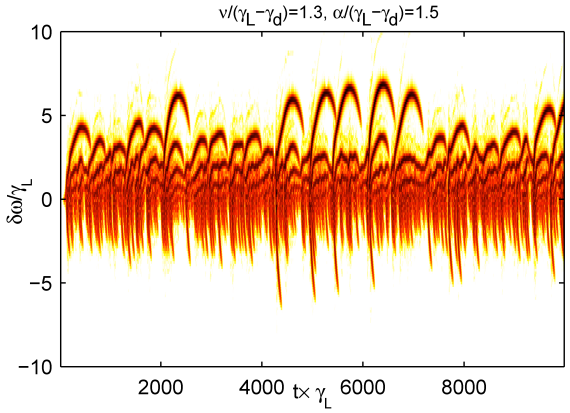

FIG. 4. Hooked frequency spectrum of holes and clumps represents interplay of drag and diffusive collisions.

The presence of drag and velocity space diffusion adds interesting new features to the behaviour of holes and clumps [7]. The drag alone breaks the symmetry of the sweeping pattern. The source term in the drag collision operator acts to enhance a phase space hole and weaken, or even suppress, a phase space clump. Also, the combined effect of drag and velocity space diffusion can produce a repetitive pattern of hooked frequency chirping shown in *FIG. 4*. The effects of drag and diffusion on a single hole can be illustrated by a simple set of coupled nonlinear differential equations derived and examined in Ref. [7]:

$$\delta\omega\omega_B = (16/3\pi^2)\gamma_L g \tag{7}$$

$$(3\pi^2/48)\omega_B^3 = g\left(\alpha^2 + d\delta\omega/dt\right) \tag{8}$$

$$\frac{dg}{dt} + \frac{\nu^3}{1.84\left(3\pi^2/48\right)^{2/3}\omega_B^2} g = \alpha^2 + \frac{d}{dt}\delta\omega \tag{9}$$

The functions to be found from this set are ω_B, $\delta\omega$, and g, where ω_B (the resonant particle bounce frequency) determines the wave amplitude, and the width of the hole, $\delta\omega$ is the mode frequency shift, and g characterizes the hole depth. The first two equations represent the wave dispersion relation and the energy balance conditions. The last equation describes a competition between the hole deepening due to drag and frequency sweeping and the hole filling via velocity space diffusion. The solution of Eqs. (7)-(9) exhibits the same qualitative trends as the results of full-scale simulations, including reproduction of the hooked spectra.

4. Long-range frequency sweeping

The initial theory for phase space holes and clumps was limited to the case of small frequency deviations from the bulk plasma eigenfrequency [6]. However, there are multiple experimental observations of frequency sweeping events in which the change in frequency is comparable to the frequency itself [8-10]. Interpretation of such dramatic phenomena requires a non-perturbative theoretical formalism. Given that the energetic particle density is usually much smaller than the bulk plasma density, it seems difficult for these particles to change the eigenmode frequency significantly. The way to resolve this difficulty is to take into account that a small but coherent group of energetic particles can still produce an observable signal with a frequency different from the bulk plasma eigenfrequency. A relevant example is a

modulated beam in the plasma. The initial modulation occurs spontaneously at the plasma eigenmode frequency. However, as the coherent structure evolves due to dissipation, the trapped particles slow down without losing coherency, and the resulting frequency shifts considerably from the initial frequency. The corresponding theoretical building block is then a nonlinear Bernstein-Greene-Kruskal (BGK) mode [11]. In Ref. [12], a rigorous solution of this type has been obtained for a bump-on-tail model with the following form of the perturbed electrostatic potential φ:

$$\varphi \equiv -\frac{1}{|e|}U\left[x - s(t);t\right], \tag{10}$$

where e is the electron charge, and the electron potential energy U is a periodic function of its first argument $\left[x - s(t)\right]$ and a slowly varying function of the second argument t. Also, the wave phase velocity $\dot{s} \equiv ds(t)/dt$ is a slowly varying function of time with a sweeping rate $\ddot{s}$. The perturbed cold electron density is linear in φ whereas the perturbation of the fast electron tail is nonlinear, dominated by adiabatic response of the trapped particles. Evaluation of this nonlinear response involves the notion that the electron distribution function is nearly uniform within the trapped particle phase space area and that the ambient passing particles remain unperturbed. The resulting Poisson equation for the BGK mode has the form

$$\frac{\partial^2 U}{\partial z^2} = -\frac{U\omega_p^2}{\dot{s}^2} - \left\{8\pi e^2\left[F_0(\dot{s}_0) - F_0(\dot{s})\right]\sqrt{\frac{2}{m}}\right\}\left[\sqrt{(U_{\max} - U)} - \left\langle\sqrt{(U_{\max} - U)}\right\rangle\right], \tag{11}$$

where $z \equiv x - s(t)$, $\dot{s}_0$ is the initial phase velocity of the wave, and angular brackets denote averaging over the spatial period λ. The maximum value, $U_{\max}$, of the potential energy is related to $\dot{s}$ by solvability condition for Eq. (11). Equation (11) gives the following structure for the BGK mode [12]:

$$U = \frac{m\dot{s}^2}{2}\left\{\frac{32\pi e^2\dot{s}\left[F_0(\dot{s}_0) - F_0(\dot{s})\right]}{3m\omega_p^2\cos\alpha}\right\}^2\left\{\frac{1+2\cos^2\alpha}{2} - \frac{3\sin 2\alpha}{4\alpha} - \left[\cos\alpha - \cos\frac{2\alpha z - \alpha\lambda}{\lambda}\right]^2\right\} \tag{12}$$

$$\alpha \equiv \omega_p\lambda/4\dot{s}$$

For small deviations of $\dot{s}$ from $\dot{s}_0$ (early phase of frequency sweeping), Eq.(12) reproduces the result of Ref. [6]. On the other hand, Eq. (12) shows that the amplitude and the mode structure change significantly for larger variations of $\dot{s}$. As a result, the boundary (separatrix) between the passing and trapped particles changes its shape as shown in *FIG. 5*. The separatrix shrinks and releases some of the originally trapped particles. The particles that remain trapped move to lower velocities and supply energy to the wave. The power extracted from the fast particle population is

$$P = -\left[F_0(\dot{s}_0) - F_0(\dot{s})\right]2m\dot{s}^2\lambda\left|\frac{32\pi e^2\dot{s}\left[F_0(\dot{s}_0) - F_0(\dot{s})\right]}{3m\omega_p^2\cos\alpha}\right|\left[\frac{\sin\alpha}{\alpha} - \cos\alpha\right]\frac{d\dot{s}}{dt} \tag{13}$$

and the balance between this power and the power dissipated in the bulk plasma determines the rate of sweeping needed to compensate for collisonal dissipation of the BGK-mode.

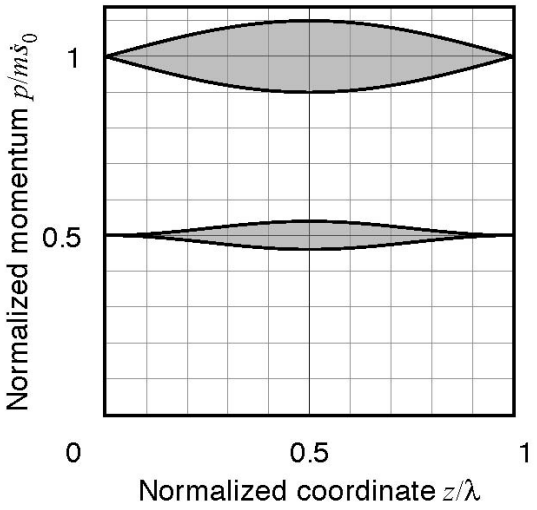

FIG. 5. Evolution of the phase-space bucket during sweeping event. The plot shows the initial separatrix (upper shaded area) and the shrinked separatrix at half of the initial mode phase velocity (lower shaded area).

Early in time, the power balance condition reproduces the square root scaling given by Eq. (6). Later in time, the mode phase velocity $\dot{s}$ deviates gradually from this simple scaling. This evolution can be viewed as transformation of the initial plasma wave into an energetic particle mode. It also presents a plausible scenario for energetic particle modes generated by Alfvén wave instabilities [13-15], for which nonlinear modification of the mode structure is essential.

The presented consideration of the 1-D electrostatic bump-on-tail problem suggests a similar approach to the frequency sweeping events in tokamaks. Experimentally, such events can be attributed to the resonant excitation of toroidal Alfvén eigenmodes. For a linear mode, the resonance condition has the form

$$\omega - n\omega_\varphi(P_\varphi;P_\theta;P_\psi) - l\omega_\theta(P_\varphi;P_\theta;P_\psi) = 0\,, \qquad (14)$$

where ω is the mode frequency, $\omega_\varphi(P_\varphi;P_\theta;P_\psi)$ and $\omega_\theta(P_\varphi;P_\theta;P_\psi)$ are the toroidal and poloidal transit frequencies, and n and l are integers. The pairs $(P_\varphi;\varphi)$, $(P_\theta;\theta)$, and $(P_\psi;\psi)$ are the canonical action-angle variables for the integrable unperturbed motion. The third pair $(P_\psi;\psi)$ describes fast gyro-motion that does not resonate with shear Alfvén perturbations. For an isolated linear resonance, the perturbed particle Hamiltonian is a sinusoidal function of $\omega t - n\varphi - l\theta$. Similarly to the bump-on-tail problem, transition to the nonlinear case generalizes the Hamiltonian to

$$H = H_0 + U\left(\int_0^t \omega(\tau)d\tau - n\varphi - l\theta;t\right), \qquad (15)$$

where the function U (to be determined numerically) is still periodic (but not necessarily sinusoidal) function of its first argument. We now note that the quantities P_ψ and $P = lP_\varphi - nP_\theta$ are constants of motion for such Hamiltonian and that slow evolution of the function U should also preserve an adiabatic invariant for trapped particles. These three conservation laws establish a simple relationship between the trapped particle distributions at any two locations of the resonance (see *FIG. 6*).

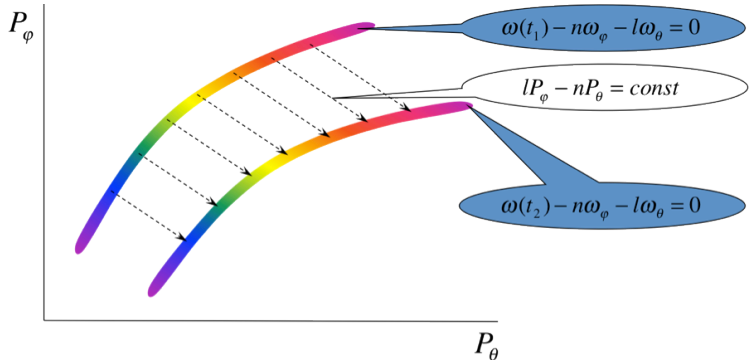

FIG. 6. Transport of resonant particles during frequency sweeping. The coloured areas are snapshots of the moving resonant region in the momentum space. The colours mark different values of the particle distribution function. The trapped particles form a locally flat distribution across the resonance and preserve the value of their distribution function when the resonance carries them along the dashed lines.

Any macroscopic quantity, like perturbed energetic particle pressure, now becomes a known functional of the unperturbed distribution and the "potential energy profile" U. What remains to be solved (numerically) is a set of linear MHD equations for bulk plasma response with an analytic nonlinear input from the energetic particles. These equations represent an analogue of Eq. (11), and their solution determines the wave profile U. After that, the power balance condition can be used to calculate the frequency-sweeping rate.

This work was funded by the U.S Department of Energy Contract No. DE-FG03-96ER-54326, by the Swedish Research Council, EURATOM, and by RCUK Energy Programme.

References

[1] BERK, H.L., BREIZMAN, B.N., PEKKER, M.S., Phys. Rev. Letters **76** (1996) 12567.
[2] CHIRIKOV, B.V., Phys. Reports **52** (1979) 263.
[3] BREIZMAN, B.N., et al., Phys. Plasmas **4** (1997) 1559.
[4] LILLEY, M.K., BREIZMAN, B.N., SHARAPOV, S.E., Phys. Rev. Letters **102** (2009), 195003.
[5] FASOLI A., et al., Phys. Rev. Letters **81** (1998) 5564.
[6] BERK, H.L., BREIZMAN, B.N., PETVIASHVILI, N.V., Phys. Letters A **234** (1997) 213, ibid **A 238** (1998) 408.
[7] LILLEY, M.K., BREIZMAN, B.N., SHARAPOV, S.E., *Effect of dynamical friction on nonlinear energetic particle modes*, to be published in Phys. of Plasmas **17** (2010).
[8] GRYAZNEVICH, M.P., SHARAPOV, S.E., Nucl. Fusion **46** (2006) S942.
[9] MASLOVSKY, D., LEVITT, B., MAUEL, M.E., Phys. Plasmas **10** (2003) 1549.
[10] FREDRICKSON, E.D., et al., Phys. Plasmas **13** (2006) 056109.
[11] BERNSTEIN, I.B., GREENE, J.M., KRUSKAL, M.D., Phys. Rev. **108** (1957) 546.
[12] BREIZMAN, B.N., Nucl. Fusion **50** (2010) 084014.
[13] CHEN, L., Plasma Phys. Control. Fusion **50** (2008) 124001.
[14] CHEN L., Phys. Plasmas **1** (1994) 1519.
[15] ZONCA F., et al., Nucl. Fusion **45** (2005) 477.